Radiation Heat Transfer in Imaging Infrared Spectrometer

A. Jhaveri, M. Kushare and A. Bhargav*
Indian Institute of Technology Gandhinagar, Gandhinagar, India - 382355
*Corresponding author: Dr. Atul Bhargav, Energy Systems Research Laboratory, IIT Gandhinagar, Palaj, Gandhinagar GJ 382355 INDIA. Email: atul.bhargav@iitgn.ac.in

Abstract:
Imaging Infrared Spectrometer (IIRS) is a Hyperspectral optical imaging [Appendix 1] instrument which measures the spectra of a scene in high resolution within spectral bands covering Near Infrared (NIR) to Mid Infrared (MIR) regions. Radiation entering the spectrometer assembly governs the temperature of different internal parts and hence plays an important role in determining the desired spectral resolution of the scene. Here an effort has been made to closely speculate the temperatures and heat fluxes inside the spectrometer assembly and understand their inter-dependency using COMSOL Multiphysics. Geometrical Ray Optics coupled with Heat Transfer physics has been used to simulate the system assembly operating at cryogenic temperatures. The current simulation investigates the variation of dependent parameters for source power of 1000 mW.

Keywords: Spectrometer, Ray Optics, Heat Transfer, Radiation

1. Introduction

Optical spectrometers have been of interest in remote sensing because of their ability to decipher an image scene based on its spectrum. Spectrometer generally consists of fore-optics, glass window, cold shield, Order Sorting Filters (OSF), Focal Plane Arrays (FPA) and cryo-cooler. It is divided into parts: Fore optics & Integrated Detector Dewar Cooling Assembly (IDDCA). Since weight constraints are of prime importance in payload design, optimum size of cryo-cooler must be known. The cooling load depends on the ability of assembly's parts to absorb, transmit and radiate energy emanating from distant scene and incident on spectrometer's aperture. The experimentation with small scale components is particularly expensive and requires sophisticated measuring and calibrating instruments [1]. Moreover the FPA has to be maintained at low temperatures (90 K) in order to achieve the desired signal to noise ratio [2].

Frequency and temperature dependent properties of OSF predominantly affects thermal load on detector arrays. Filter bands are joined together with opaque chromium masking. This reduces the flux on detector array and lost area is expected to be formed beneath filter joints. The amount and location of reduction of flux can be found from computational results which would otherwise be difficult to measure experimentally. Multiphysics approach in the simulation helps in the understanding of thermal analysis better and draws attention to subtleties involved.
The optical designs, diffraction grating in fore-optics, system specification and experimental results of HyTES - Hyperspectral Thermal Emission Spectrometer of Jet Propulsion Laboratory (JPL) have been discussed in detail by W. R. Johnson et al [3]. K. D. Stout et al [4] has discussed the thermal and structural design of the REgolith X-ray Imaging Spectrometer (REXIS). They have used computer simulations for spectrometer's thermal design and have speculated the average power consumption by the cooler. Gabriele E. Arnold et al [5] has discussed the thermal design and performance of MERTIS- ESA's Mercury planetary orbiter spacecraft mission with special focus on the design of fore-optics geometry.
This paper is an attempt to develop a computational study which can simulate the thermal parameters of an assembly at extremely low temperatures. A computational study has been carried out for the IDDCA in the spectral range of 0.8 to 5 μm using Ray Optics and Heat Transfer modules of COMSOL Multiphysics®.

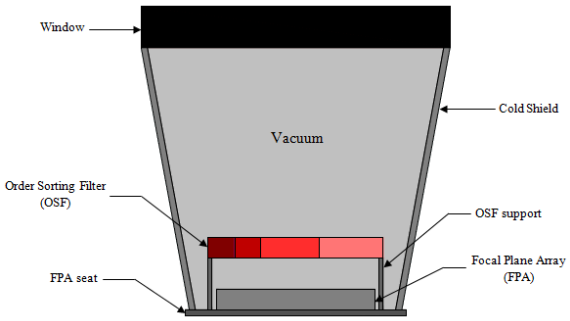

Figure 1: A typical Integrated Detector Dewar Cooling assembly (IDDCA)

Spectral distribution of wavelengths can be achieved by designing OSF which is made up of semi-transparent material sapphire (Al_2O_3) that has an excellent working capability in low temperature environment. Rays incident on detector array generate electrons proportional to the heat flux which are further received by camera electronics. Camera post-processing then generates scene of an image on image plane. Thus it is important to regulate heat flux and temperature of detector array.

2. Use of COMSOL Multiphysics®

Ray optics coupled with Heat Conduction in solids and Surface to Surface Radiation has been modeled separately to calculate resultant incident flux on detector array. The propagation of rays inside Dewar assembly is modeled using Snell's law, Fresnel equations and eikonal equations while Radiative Transfer Equation (RTE) is used for solving surface to surface radiation heat transfer. Semi-transparent media such as glass window and OSF having wavelength dependent refractive indices different than surrounding medium also take part in radiation. This phenomenon has been modeled using radiation in participating media interface by Discrete Ordinate Method (DOM). Rays undergo attenuation in semi-transparent media and heats up the domain which acts as a heat source.

2.1 Mathematical modeling

In order to evaluate radiative flux on a surface, radiative intensity for all directions and wavelengths must be known. The intensity inside a participating media can be determined from Radiative Transfer Equation (RTE) [6].

$$\frac{\partial I_\eta}{\partial s} = k_\eta I_{b\eta} - k_\eta I_\eta - \sigma_{s\eta} I_\eta + \frac{\sigma_{s\eta}}{4\pi}\int_{4\pi} I_\eta(\hat{\mathbf{s}}_i)\Phi_\eta(\hat{\mathbf{s}}_i,\hat{\mathbf{s}})d\Omega_i \qquad (1)$$

where: c is the speed of light, I is the intensity of light, $k_\eta$is absorption coefficient, j_η is emission coefficient, $\sigma_{s\eta}$ is scattering coefficient, Φ_η is scattering phase function and Ω_i is solid angle. The terms on right side depicts, how intensity is enlarged by emission ($k_\eta I_{b\eta}$) reduced by absorption ($k_\eta I_\eta$) and scattering. For a non participating medium

$$k_\eta = \sigma_{s\eta} = 0 \quad or \quad I_\eta(\hat{s}) = \text{constant} \qquad (2)$$

When a ray propagates through a strongly absorbing medium with a considerable part of imaginary refractive index of the material, it undergoes attenuation within the domain. Imaginary part of refractive index is responsible for the extent of attenuation which causes temperature rise in the domain.

$$\frac{dQ_{src}}{dt} = -\frac{1}{V_j}\sum_{j=1}^{N}\frac{\partial Q_j}{\partial t}\int \delta(r - q_j)dV \qquad (3)$$

where: δ is a Dirac function, V is volume of an element and Q_{src} is a source power. The deposited ray power in the domain increases by an amount equal in magnitude to the power lost by the ray but opposite in sign.

The ray trajectory can be computed by solving six coupled first-order ordinary differential equations (4-6) for the components of **k** (wave vector) and **q** (position vector).

$$\frac{d\mathbf{k}}{dt} = -\frac{\partial\omega}{\partial\mathbf{q}} \qquad \frac{d\mathbf{q}}{dt} = \frac{\partial\omega}{\partial\mathbf{k}} \qquad (4)$$

In regions of constant refractive index, the simplified equations of motion are

$$\frac{d\mathbf{k}}{dt} = 0 \qquad \frac{d\mathbf{q}}{dt} = \frac{c|\mathbf{k}|}{n} \qquad (5)$$

The **k** (wave vector) and ω (angular frequency) can be expressed in terms of the ψ (phase).

$$\mathbf{k} = \frac{\partial\psi}{\partial\mathbf{q}} \qquad \omega = -\frac{\partial\psi}{\partial t} \qquad (6)$$

2.2 Computational modeling

The 3D model geometry is shown in Figure 2. It consists of window, cold shield, OSF, OSF support, FPA and FPA seat. FPA is a highly sensitive detector array made of photovoltaic HgCdTe (Mercury Cadmium Tellurium) to 0.8 to 5 μm spectral ranges. Cold Shield protects FPA from unwanted heating by thermal

radiation. OSF allows only wavelength band of interest to pass through it. The incident radiation on FPA is being optimized by window. FPA seat is directly connected to the cold finger which provides cooling to the assembly and acts as a heat sink.

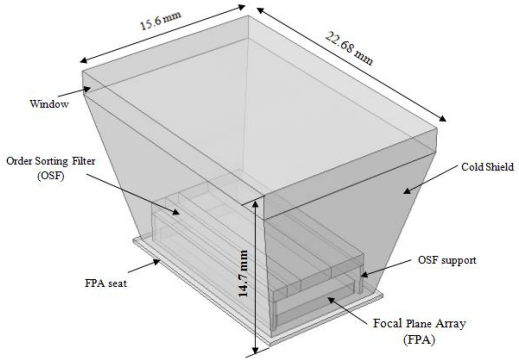

Figure 2: IDDCA configuration

The bottom pane of window, inner walls of cold shield, surfaces of OSF and top surface of FPA are treated diffused as they radiate energy due to their surface temperature without any directional variation in their radiative properties. The FPA is to be maintained at 90 K by a passive cryo-cooler through cold finger. Assuming the conductivity of cold finger to be very high, the FPA seat is maintained at 90 K. Temperature of Spectrometer (SM) assembly also affects the IDDC assembly's temperatures and fluxes. To compensate for the probable uncertainty, IDDCA has been tested for three different SM assembly's temperatures of 253 K, 273 K and 293 K.

Table 1: Material list for IDCA's parts

Sr. No.	Part	Material	Remark
1	Glass window	Sapphire	Transmissive
2	Cold shield	Aluminium	Inside surface-black paint
3	OSF	Sapphire	Transmissive
4	OSF support	Aluminium	Inside surface-black paint
5	FPA	Ceramic (HgCdTe)	Emissive
6	FPA seat	Aluminium	Highly conductive

2.3 Meshing of model

The best grid size of domain should be verified for the optimal computational studies. For the computation to be within the asymptotic range small GCI is an indicator. Firstly a grid which can be considered fine is selected and then creating coarser grids consequently by reducing the cell count by half i.e. if the fine grid has a cell count of 0.5 million, and then a coarser grid of 0.25 million and 0.125 million should be generated subsequently.

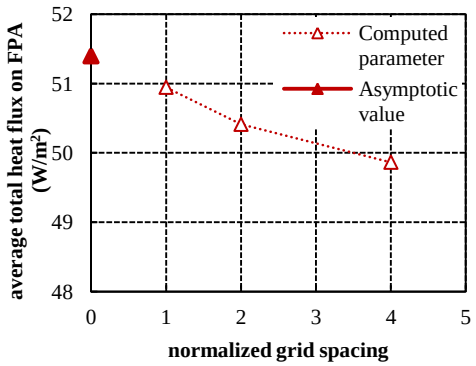

Figure 3: Mesh convergence study

Figure 3 shows the variation of average total heat flux on FPA with normalized grid spacing used for the computation. GCI for mesh count 0.25 million came out to be 2% which indicates the solution is within the asymptotic range and this mesh size was selected for the further study. Tetrahedral mesh was used with 0.2 mm maximum size and 0.045 mm minimum size. Mesh view is shown in Figure 4.

Figure 4: IDDCA mesh view

3. Results and Discussions

This section discusses the results obtained from ray tracing and heat transfer studies. Radiative intensities are plotted for the surfaces according to their roles in computation of irradiation on FPA surface. Since rays come from distant objects, all rays are assumed to be parallel. Rays passes through the spectrometer assembly's fore-optics before they enter IDDCA. Window made up of sapphire has an average refractive index of 1.7845. Initial intensity of rays entering IDDCA is assumed to be 1000 W/m^2.

3.1 OSF top surface irradiation

The top surface of OSF receives radiation from inner walls of cold shield and bottom pane of window. Symmetry in the irradiation is expected and can be observed in Figure 5.

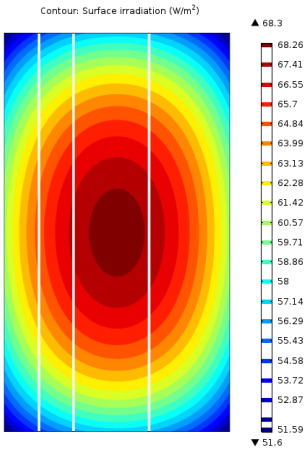

Figure 5: OSF irradiation (W/m^2)

3.2 FPA irradiation

It is important to know the temperature and heat flux incident i.e. irradiation on the FPA surface because this is where core of the problem lies. It can be noted that irradiation on FPA on area beneath chromium joints is higher than other area. This is due to the fact that in-spite of having lower emissivity than sapphire, higher temperature at joint area emits lesser radiative flux and eventually higher irradiation on FPA in that region. The total average radiative heat flux is 18 W/m^2.

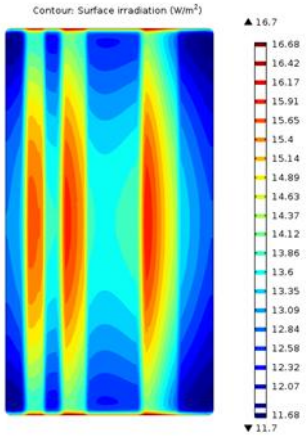

Figure 6: FPA surface irradiation

3.3 FPA temperature

Temperature distribution on FPA due to surface to surface transfer follows the same reasoning as of irradiation on FPA. The average temperature of FPA is measured to be 104.2 K.

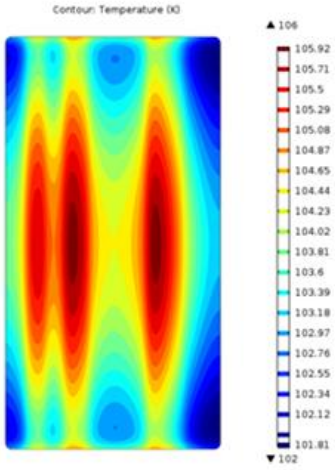

Figure 7: FPA temperature

The main aim of doing ray tracing study is to be able to perform spectral screening of wavelengths and calculate conductive heat flux. This can be achieved by using frequency dependent refractive index (imaginary part). Imaginary part of refractive index is responsible for attenuation of rays in absorbing media. A ray trace for the whole assembly is shown in Figure 8. The total average conductive heat flux is measure to be 1070 W/m^2.

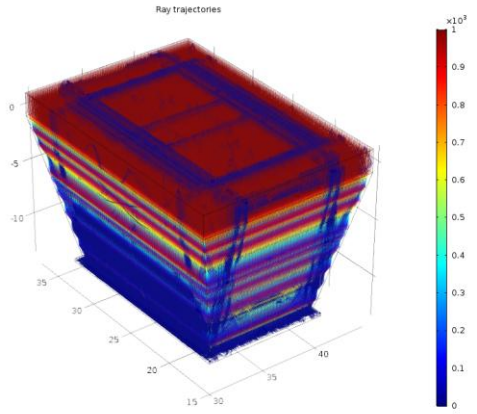

Figure 8: Ray trajectories

Irradiation on FPA surface is a cumulative sum of heat fluxes in two cases.

Irradiation on FPA = Radiative heat flux + conductive heat flux

$= 18 + 1070\ W/m^2$

$= 1088\ W/m^2$

Thus total irradiation on FPA comes out to be 122 mW.

4. Conclusions

This section deals with the important derivation from the work done and concluding remarks. As stated in the modeling part, total incident radiation on detector array is added while temperature conditions are logically deduced. Simulation results have helped to understand the phenomenon of radiation heat transfer better in such a small geometry. Irradiation on focal plane and temperature of detector array due to order sorting of wavelengths was an important expectation from the simulations which has been duly addressed with convincing results.

5. References

1. K. D. Stout and R. A. Masterson, "Thermal design and performance of the REgolith x-ray imaging spectrometer (REXIS) instrument," Proc. SPIE - Int. Soc. Opt. Eng., vol. 9150, p. 91501J, 2014.
2. SciTech Team and VIRTIS Team, "Virtis: Visible and Infrared Thermal Imaging Spectrometer," *Venus Express webpage, ESA Publ.*, (2013).
3. W. R. Johnson, S. J. Hook, P. Mouroulis, D. W. Wilson, S. D. Gunapala, V. Realmuto, A. Lamborn, C. Paine, J. M. Mumolo, and B. T. Eng, "HyTES: Thermal imaging spectrometer development," *IEEE Aerosp. Conf. Proc.*, vol. 91109, no. 818, pp. 1–8, 2011.
4. K. D. Stout and R. A. Masterson, "Thermal design and performance of the REgolith x-ray imaging spectrometer (REXIS) instrument," *Proc. SPIE - Int. Soc. Opt. Eng.*, vol. 9150, p. 91501J, 2014.
5. G. E. Arnold, J. Helbert, H. Hiesinger, H. Hirsch, E. K. Jessberger, G. Peter, and I. Walter, "Mercury radiometer and thermal infrared spectrometer-a novel thermal imaging spectrometer for the exploration of Mercury," *J. Appl. Remote Sens.*, vol. 2, p. -, 2008.
6. M.F.Modest, "RTE in participating media," in *Radiative Heat Transfer*, Academic Press, 2013, pp. 279–302.

6. Acknowledgements

We acknowledge the support received from our lab mates at ESRL and friends at IIT Gandhinagar. COMSOL License No. 16075953

7. Appendix [I]

Hyperspectral Imaging

Hyperspectral imaging is an imaging technique which collects and processes data from across electromagnetic spectrum. It obtains information for each pixel present in the image scene for identifying material or detection purpose. It divides the spectra of image scene into number of bands and each band is mapped into contiguous spectrum. Hyperspectral imaging covers wide spectra including short wave infrared (SWIR), near infrared (NIR) and mid wave infrared (MWIR). Objects have their unique identification fingerprints in electromagnetic spectrum based on its characteristic to absorb certain wavelengths. A normal multispectral image has 3-10 bands whereas a typical Hyperspectral image has more than 200 bands. Hyperspectral images have numerous applications in oil & gas, agricultural, remote sensing, healthcare and astronomical studies.